



The BLIMP1—EZH2 nexus in a non-Hodgkin lymphoma

Kimberley Jade Anderson^{1,2,3} · Árný Björg Ósvaldsdóttir^{1,2,3} · Birgit Atzinger^{1,2,3} · Gunnhildur Ásta Traustadóttir^{1,3} · Kirstine Nolling Jensen^{3,4,5} · Aðalheiður Elín Lárusdóttir^{1,2,3} · Jón Thór Bergthórsson^{2,3,6} · Ingibjörg Hardardóttir^{3,4,5} · Erna Magnúsdóttir^{1,2,3}

Received: 27 May 2019 / Revised: 26 May 2020 / Accepted: 1 June 2020 / Published online: 12 June 2020
© The Author(s), under exclusive licence to Springer Nature Limited 2020

Abstract

Waldenström's macroglobulinemia (WM) is a non-Hodgkin lymphoma, resulting in antibody-secreting lymphoplasmacytic cells in the bone marrow and pathologies resulting from high levels of monoclonal immunoglobulin M (IgM) in the blood. Despite the key role for BLIMP1 in plasma cell maturation and antibody secretion, its potential effect on WM cell biology has not yet been explored. Here we provide evidence of a crucial role for BLIMP1 in the survival of cells from WM cell line models and further demonstrate that BLIMP1 is necessary for the expression of the histone methyltransferase EZH2 in both WM and multiple myeloma cell lines. The effect of BLIMP1 on EZH2 levels is post-translational, at least partially through the regulation of proteasomal targeting of EZH2. Chromatin immunoprecipitation analysis and transcriptome profiling suggest that the two factors co-operate in regulating genes involved in cancer cell immune evasion. Co-cultures of natural killer cells and cells from a WM cell line further suggest that both factors participate in immune evasion by promoting escape from natural killer cell-mediated cytotoxicity. Together, the interplay of BLIMP1 and EZH2 plays a vital role in promoting the survival of WM cell lines, suggesting a role for the two factors in Waldenström's macroglobulinaemia.

Introduction

Waldenström's macroglobulinemia (WM) is a rare plasma cell dyscrasia with 3–6 people per million diagnosed

annually world wide [1–3]. It is characterised by the expansion of a monoclonal population of malignant cells in the bone marrow with a lymphoplasmacytic character, that is, cellular phenotypes ranging from that of B-lymphocytes to overt plasma cells that exhibit hypersecretion of immunoglobulin M (IgM) [4]. A large proportion of WM symptoms arise because of high levels of IgM paraprotein in patients' blood and tissues [5]. Curiously, over 90% of WM tumours carry an activating mutation in the signalling adaptor MYD88, typically L265P that serves as a key oncogenic driver in the disease [6–8].

The transcription factor B-lymphocyte induced maturation protein-1 (BLIMP1) drives plasma cell differentiation, mediating transcriptional changes via the recruitment of co-factors to chromatin [9–11]. During plasma cell maturation, BLIMP1 represses key B-lymphocyte identity factors and signalling mediators [12, 13], while simultaneously driving plasma cell specific gene expression and antibody secretion [14–16]. Depending on the mouse model, BLIMP1 appears to be required for the survival of long-lived plasma cells in the bone marrow and promotes multiple myeloma (MM) cell survival [15, 17–19]. Conversely, BLIMP1 functions as a tumour suppressor in diffuse large B cell lymphoma (DLBCL), consistent with its repression of proliferation genes during plasma cell differentiation [14, 20–22]. WM

Supplementary information The online version of this article (<https://doi.org/10.1038/s41388-020-1347-8>) contains supplementary material, which is available to authorized users.

✉ Erna Magnúsdóttir
erna@hi.is

- 1 Department of Anatomy, Faculty of Medicine, University of Iceland, Vatnsmýrarvegur 16, 101 Reykjavík, Iceland
- 2 Department of Biomedical Science, Faculty of Medicine, University of Iceland, Vatnsmýrarvegur 16, 101 Reykjavík, Iceland
- 3 The University of Iceland Biomedical Center, Vatnsmýrarvegur 16, 101 Reykjavík, Iceland
- 4 Department of Biochemistry and Molecular Biology, Faculty of Medicine, Vatnsmýrarvegur 16, University of Iceland, 101 Reykjavík, Iceland
- 5 Department of Immunology, Landspítali-The National University Hospital of Iceland, Hringbraut, 101 Reykjavík, Iceland
- 6 Department of Laboratory Haematology, Landspítali-The National University Hospital of Iceland, Hringbraut, 101 Reykjavík, Iceland

tumours harbour frequent heterozygous losses of *PRDM1*, the gene encoding BLIMP1 [23]. However, BLIMP1 is expressed in a subset of WM lymphoplasmacytic cells [24, 25], in line with its necessity for antibody secretion [16, 18, 26], a critical aspect of WM pathology. Furthermore, BLIMP1 is induced downstream of toll like receptor engagement of MYD88 [27, 28] and *PRDM1* mRNA is elevated in tumours harbouring the MYD88^{L265P} mutation [29], which is associated with poorer prognosis in WM [30].

Also important in plasma cell differentiation, enhancer of zeste 2 (EZH2) is both a physical and genetic interaction partner of BLIMP1 [16, 31]. The interaction was first suggested in mouse primordial germ cells, where BLIMP1 and EZH2 share a highly overlapping set of binding sites [32, 33]. EZH2 is the catalytic component of the polycomb repressive complex 2, placing methyl groups on lysine 27 of histone 3, typically tri-methylation (H3K27me3), to repress transcription [34, 35]. While EZH2 is essential for embryonic development [36], it has frequent activating mutations in DLBCL, and is commonly overexpressed in MM, making it a promising therapeutic target [37–39]. While aberrant regulation of histone modifications has been implicated in WM pathogenesis [40], the role of EZH2 is yet to be investigated.

In this study, we examine the potential role of BLIMP1 in WM and its interplay with EZH2 using available cell line models of the disease. We demonstrate for the first time that BLIMP1 promotes the survival of WM cells from these models and maintains EZH2 protein levels. We identify a large overlap in the targets of the two factors and show that they repress transcription of an overlapping set of genes in a parallel fashion. In a highly novel finding, we reveal roles for BLIMP1 and EZH2 in evasion from natural-killer (NK) cell mediated cytotoxicity, with BLIMP1 suppressing NK cell activation in response to cells from a WM cell line, and both factors suppressing NK cell mediated WM cell death, potentially implicating the factors in immune evasion. In sum, our data highlight the multifaceted roles of the BLIMP1-EZH2 nexus in promoting the survival of cells from a WM cell line and may suggest a more general mechanism for these factors' interplay in other tumour types such as MM, where they are co-expressed.

Results

BLIMP1 is important for cell survival in Waldenström's macroglobulinemia

BLIMP1 is expressed in a subset of WM patients' lymphoplasmacytic cells [24, 25]. Therefore, given its crucial roles in antibody secretion and plasma cell differentiation, we wanted to determine whether it plays a role in WM cell

biology. We compared BLIMP1 expression in the myeloma cell line OPM-2 [41] to that of three WM cell lines RPCI-WM1 (RP), MWCL-1 (MW) and BCWM.1 (BC) by immunofluorescence staining (Fig. 1a). All of the RP cells expressed BLIMP1, while the MW and BC cells had more heterogeneous expression, with 43 and 18% of the cells expressing high levels of BLIMP1, respectively, (Fig. 1a right panel). We subsequently focused mainly on the RP cell line as it had the most uniform BLIMP1 expression.

To knock-down (KD) BLIMP1, we engineered RP cells with two distinct doxycycline (dox)-inducible artificial miRNAs targeting *PRDM1* mRNA (*PmiR1* and *PmiR2*), or a non-targeting control miRNA (*NTmiR*), and MW cells with *NTmiR* and *PmiR1*. The induction of *PmiR1* and *PmiR2* led to the loss of BLIMP1 protein in RP cells (Fig. 1b) and *PmiR1* led to a 60% reduction in MW cells (Fig. 1c). The KD resulted in decreased cell survival, with 58 and 72% live cells remaining relative to *NTmiR* in RP *PmiR1* and *PmiR2* cell cultures respectively, 48 h post dox addition (Fig. 1d). No viable cells remained 6 days after induction of *PmiR1* or *PmiR2* (Fig. S1A). MW *PmiR1* cells also displayed an initial decrease in viability to 71% of the *NTmiR* (Fig. 1d), but by day 5 had recovered their viability, perhaps due to the survival of the non-BLIMP1 expressing cellular compartment. The proportion of apoptotic cells increased in RP cells by 2.6- and 2.3-fold 48 h post *PmiR1* and *PmiR2* induction respectively (Fig. S1B). Although we consistently saw an increase in Annexin-V positive MW cells upon BLIMP1-KD, it was not statistically significant (Fig. S1C).

Crucially, the decreased cell viability upon BLIMP1-KD in RP cells was rescued in *PmiR1* cells transduced with miR-resistant BLIMP1 from a lentiviral construct [42] (Fig. 1e, S1D-F). BLIMP1 overexpression resulted in 81–101% viability, relative to BLIMP1-transduced *NTmiR* control, whereas EGFP-transduced cells were 65–106% viable at 48 h post *PmiR1* induction (Fig. 1f and S1D-F). However, 5 days post BLIMP1 KD, 57–75% of the BLIMP1-transduced cells were viable, compared with only 3–20% of the EGFP-transduced cells (Fig. 1f), similar results were obtained with *PmiR2* (Fig. S1E). This was further reflected in an increased reduction capacity of the BLIMP1 complemented cells (23% vs. 6% resazurin reduction) (Fig. 1g). Taken together, BLIMP1 is a survival factor in RP and MW cells, likely due to the suppression of apoptosis.

BLIMP1 expression maintains EZH2 protein levels

As studies of mouse plasmablasts and germ cells have shown a functional overlap and direct interaction of BLIMP1 and EZH2 [16, 32, 33], we investigated the potential interplay between the two factors in WM and MM

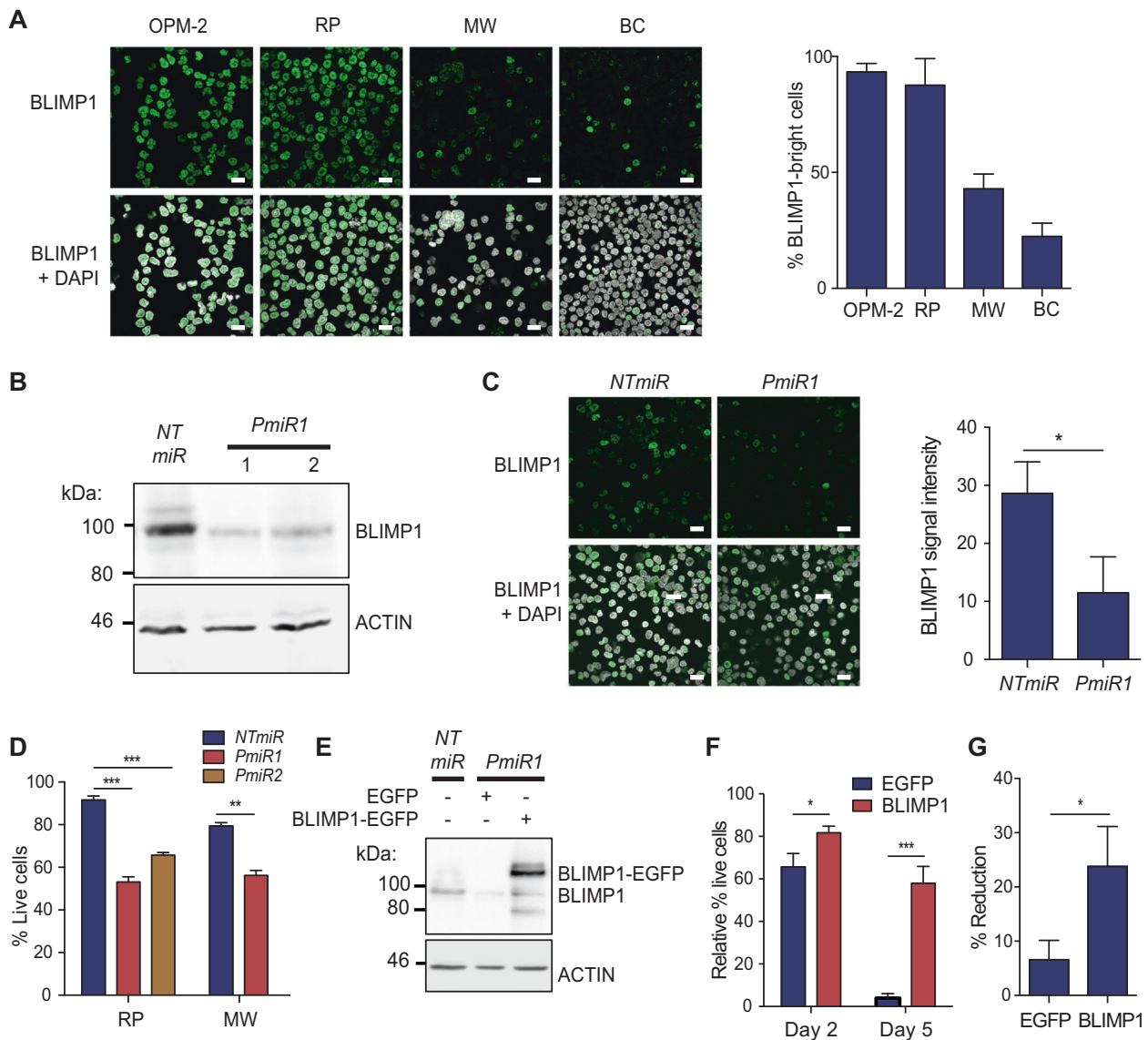


Fig. 1 BLIMP1 promotes the survival of WM cells. **a** BLIMP1 expression in the myeloma cell line OPM-2 and in WM cell lines RP, MW and BC as detected by immunofluorescence staining, with a bar graph representing percentage of BLIMP1^{bright} cells. Scale bars represent 20 μ m. **b** Representative immunoblot of BLIMP1 expression following 48 h induction of RP cells expressing *NTmiR*, *PmiR1* or *PmiR2*. **c** Immunofluorescence staining of BLIMP1 following 48 h induction in MW cells expressing *NTmiR* or *PmiR1*, with CellProfiler quantification. **d** Percentage of live cells as determined by Trypan blue exclusion assay in the RP and MW cell lines comparing *PmiR1* or *PmiR2* to *NTmiR* following 48 h of induction. **e** Immunoblot depicting lentiviral ectopic expression of EGFP or BLIMP1-EGFP in the RP *PmiR1* cells, next to the RP *NTmiR* cells. **f** The percentage of live RP

PmiR1 cells with ectopic EGFP or BLIMP1-EGFP expression determined by the Trypan blue exclusion assay normalised to the percentage of live cells following transduction of RP *NTmiR* cells with EGFP or BLIMP1-EGFP. BLIMP1-EGFP compared to EGFP at Day 2 and Day 5. **g** Percent reduction as measured by resazurin assay for RP *PmiR1* cells with EGFP compared to BLIMP1-EGFP, five days after miR induction. All *p* values as determined by student's two-tailed *t* test. **p* \leq 0.05; ***p* \leq 0.01; ****p* \leq 0.001; *****p* \leq 0.0001. All graphs were plotted as the mean of three independent experiments, with error bars representing standard deviation. The migration rates and sizes of protein size standard markers shown in kD to the left of the blots in (b) and (e).

cells. Our first line of inquiry revealed a decrease in EZH2 protein expression upon BLIMP1 KD in RP cells (Fig. 2a) and in OPM-2 MM cells also engineered with inducible *PmiR1* (Fig. 2b). Genetic complementation with miR-resistant BLIMP1 (Fig. 1e) restored EZH2 protein levels in RP cells, confirming the effect is specifically due to

BLIMP1 depletion (Fig. 2c, quantified in Fig. S2A). Furthermore, BLIMP1 and EZH2 levels were positively correlated in two separate complementation experiments ($R^2 = 0.338$, $R^2 = 0.684$) based on quantitation of nuclear fluorescent signal. Taken together these data reveal a dependency of EZH2 expression on BLIMP1.

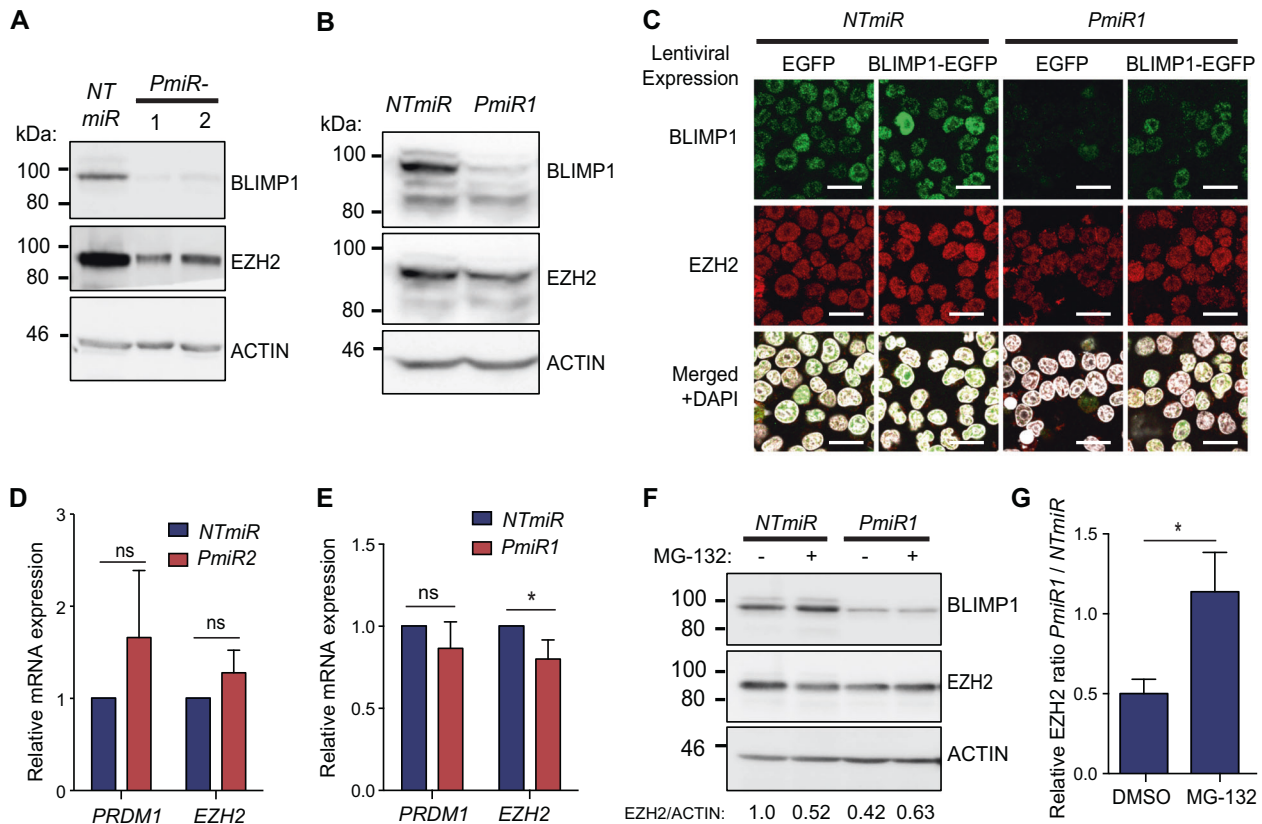


Fig. 2 BLIMP1 maintains EZH2 protein levels in WM cells. **a** An immunoblot of BLIMP1 and EZH2 expression following 48 h induction of RP cells expressing *NTmiR*, *PmiR1* or *PmiR2*. **b** An immunoblot of BLIMP1 and EZH2 expression following 48 h induction of OPM-2 cells expressing *NTmiR* compared to *PmiR1*. **c** Immunofluorescence staining of BLIMP1 and EZH2 expression following 48 h induction of RP cells expressing *NTmiR* or *PmiR1*, transduced with EGFP or BLIMP1-EGFP. Scale bars represent 20 μ m. **d** RT-qPCR results depicting relative mRNA expression of *PRDM1* and *EZH2* normalised to *PPIA* and *ACTB* in the RP cell line and **(e)** in the OPM-2 cell line. **f** An immunoblot of BLIMP1 and EZH2 expression

Reverse transcription followed by quantitative PCR (RT-qPCR) showed that *EZH2* mRNA levels were unchanged in RP *PmiR2* cells upon BLIMP1 KD and only slightly decreased in OPM-2 cells upon *PmiR1* induction, indicating that the loss of EZH2 expression is post-transcriptional (Fig. 2d, e). We also measured the levels of LSD1 and G9a, two proteins previously shown to interact with BLIMP1, as well as the NF κ B subunit p65 (Fig. S2C-D). These factors are all unchanged at the mRNA level upon BLIMP1 KD (Table S1). While we saw that EZH2 protein levels were consistently decreased upon BLIMP1 KD with both *PmiR1* as well as *PmiR2*, none of the other three proteins were reproducibly reduced between the two miRs (Fig. S2C, D), consistent with an EZH2-specific effect rather than a general increase in proteasomal activity downstream of BLIMP1. Notably, treating RP *PmiR1* cells with the proteasome inhibitor MG-132, restored EZH2 to the same level as that of MG-132-treated *NTmiR* cells (Fig. 2f, g, and Fig

following 24 h induction of *NTmiR* or *PmiR1* expression in RP cells with dox, treated with DMSO or 5 μ M MG-132 for 4 h. The numerical quantification of EZH2 levels normalized to ACTIN are shown below the blot. **g** The ratio of EZH2 expression relative to ACTIN for RP *PmiR1* cells divided by RP *NTmiR* cells treated with DMSO or MG132 as in Fig. 2f. All *p* values as determined by student's two-tailed *t* test. (ns) $p > 0.05$; $*p \leq 0.05$. All graphs were plotted as the mean of three independent experiments with error bars representing standard deviation. The migration rates and sizes of protein size standard markers shown in kD to the left of the blots in **(a)**, **(b)** and **(f)**.

S2E-F), showing that BLIMP1 modulates EZH2 by inhibition of proteasome mediated degradation.

However, complementing the RP *PmiR1* cells with ectopic EZH2 expression (Fig. S2G) failed to increase their viability (Fig. S2H). Consistent with this, the EZH2-specific catalytic inhibitor tazemetostat did not affect RP cell viability even over a 96 h period (Fig. S2B), despite a dose dependent decrease in H3K27me3 levels (Fig. S2I), nor did 7 days of treatment. Taken together, BLIMP1 maintains EZH2 protein levels via modulation of proteasome mediated degradation, but the effect of BLIMP1 on cell survival is independent of EZH2.

BLIMP1 KD induces large transcriptional changes

To investigate the overlap of BLIMP1 and EZH2 in downstream gene regulation in WM cells, we performed transcriptome profiling of the RP *PmiR2* and *NTmiR* cells

following 48 h of induction. Using a q value cutoff of 0.05, we identified 7814 differentially expressed genes between *PmiR2* and *NTmiR* (Fig. 3a and Table S1).

Consistent with BLIMP1 repressing the B cell transcriptional program [14, 16, 18, 43], previously characterised targets, including *CIITA* [44, 45], *PAX5* [46], *SPIB* and *BCL6* [14] were repressed by BLIMP1 in our study (Fig. 3b). However, other BLIMP1 targets such as *MYC* [47] and *ID3* [14] were unaltered. Curiously, the myeloma-driving transcription factor *IRF4* [48], which is activated downstream of BLIMP1 in plasma cells [16] was repressed by BLIMP1 in RP cells (Fig. 3b). Interestingly, the BTK inhibitor, *IBTK* and key apoptosis genes were also repressed by BLIMP1 (Fig. 3c). We validated these results from *PmiR2*-expressing cells in *PmiR1* cells by RT-qPCR, showing that 19 out of 22 genes were reproducibly altered in *PmiR1*-expressing RP cells, including *IFNG-AS1*, an antisense transcript expressed from the *IFNG* locus (Fig S3C) [49].

In order to assess to which extent these changes were due to cell autonomous effects of BLIMP1 KD or a possible cytokine signalling loop amplified in the cultures downstream of BLIMP1 KD, we subjected unmodified RP cells to conditioned media from RP cells expressing either *NTmiR*, *PmiR1* or *PmiR2* for 48 h. A small subset of the genes tested showed modest gene expression changes, although statistically significant changes (3 and 2 out of 13 genes tested for *PmiR1* and *PmiR2* cell conditioned media, respectively) had much smaller amplitudes of change than those autonomous to the cells (Fig. S3D and Table S1). The only exception to this was *OAS2*, showing similar changes in cell conditioned media as in KD cells for *PmiR1* but not *PmiR2*. *IFNG-AS1* exhibited unaltered expression in cells cultured in both *PmiR1* and *PmiR2* conditioned media. Taken together, BLIMP1 KD induces extensive gene expression changes in RP cells including the de-repression of B cell- and apoptosis-related genes.

BLIMP1 and EZH2 regulate overlapping pathways

Because of the dependency of EZH2 on BLIMP1, we asked to which extent the effect of BLIMP1 on transcription is dependent on EZH2's catalytic activity, and performed transcriptome profiling upon catalytic inhibition of EZH2 with tazemetostat. This resulted in 450 differentially expressed genes compared to vehicle alone (Fig. 3d and Table S2). The amplitude of change for individual genes was smaller than in BLIMP1 KD (Comparing Fig. 3d, a). Nevertheless, a highly significant overlap emerged between transcripts increased in the BLIMP1 KD and tazemetostat treated cells (184 genes, $p = 1.8e-37$) (Fig. 3e, Table S3). The genes with decreased expression did not significantly overlap (Fig. 3f, Table S4). Tazemetostat led to the de-

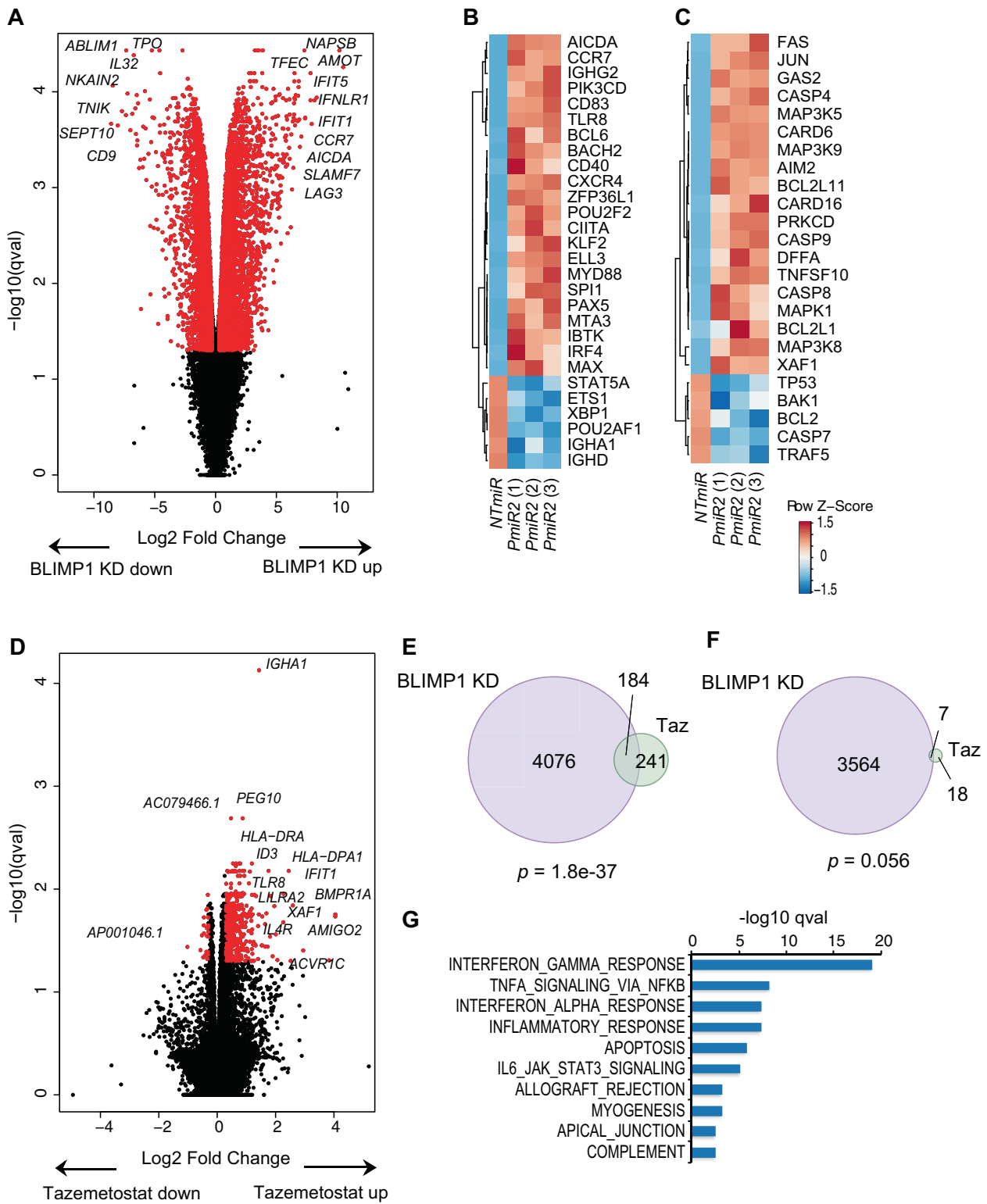
repression of B cell identity genes, including *STAT5B* and *ID3* (Fig. S3A) and, despite EZH2 inhibition not affecting cell survival, a number of apoptosis genes were differentially expressed, including *XAF1*, *CASP4*, *FAS* and *JUN* (Fig. S3B), suggesting a possible sensitisation to apoptosis.

To investigate the pathways jointly regulated by BLIMP1 and EZH2, we performed an overlap analysis using the molecular signatures database [50, 51] of the 184 genes induced by both BLIMP1 KD and tazemetostat. Several gene sets were significantly enriched, including interferon and TNF α responses, the inflammatory response and apoptosis (Fig. 3g), consistent with the known roles of BLIMP1 [13, 17, 52–54], and suggesting that pathways involved in immune responses are regulated in concert by BLIMP1 and EZH2. Collectively, the transcriptomic analyses demonstrate a large overlap in targets of repression by BLIMP1 and EZH2, highlighting the interplay of the two factors.

BLIMP1 binds to a set of H3K27me3 marked genes at a distance from the mark

Given the overlap in genome wide positioning of BLIMP1 and the H3K27me3 mark in mouse plasmablasts [16], we examined whether the overlapping effects of BLIMP1 and EZH2 on transcription could also be modulated by BLIMP1 recruiting EZH2 to chromatin in WM cells. We therefore performed chromatin immunoprecipitation coupled to deep sequencing (ChIPseq) for H3K27me3 and BLIMP1 in RP cells. We identified 14946 H3K27me3 peaks (Table S5), assigned to 4198 genes (Table S6), and 506 BLIMP1 peaks (Table S7), assigned to 841 genes (Table S8). If BLIMP1 recruits EZH2 to chromatin in WM cells, a large proportion of BLIMP1 peaks would be located in close proximity to H3K27me3 marks. However, only eight sites bore both H3K27me3 and BLIMP1 within 500 bp (Fig. 4a) and only a small level of bimodal enrichment of H2K27me3 was observed in the ± 3 kb flanking BLIMP1 peaks (Fig. 4b). However, when we compared the genes assigned to the peaks in the respective experiments, 261 genes were both bound BLIMP1 and marked by H3K27me3 in RP cells, a highly statistically significant overlap ($p = 2.9e-25$) (Fig. 4c, Table S9). An analysis [50, 51] of the genes marked by both BLIMP1 and H3K27me3 in the RP cells demonstrated significant enrichment for the same immune signalling gene sets as in the RNAseq data (Fig. S4A).

To test whether these findings apply also to MM, we performed ChIPseq for BLIMP1 and H3K27me3 in the OPM-2 (Tables S10–13) and NCI-H929 (Tables S14–17) myeloma cell lines, and EZH2 in NCI-H929 cells (Tables S18–19). As with the RP cells, we rarely observed peaks within a 500 bp distance when comparing BLIMP1 and H3K27me3 (Fig. S4B) or BLIMP1 and EZH2 (Fig. S4C).



However, we observed a statistically significant overlap between genes bound by BLIMP1 and H3K27me3 in NCI-H929 cells, but not OPM-2 cells (Fig. S4D). Genes bound both by BLIMP1 and EZH2 were not statistically over-represented in NCI-H929 cells (Fig. S4E). The above

analyses reveal that the majority of BLIMP1 and EZH2 binding to chromatin occurs at relatively distant sites both in MM and WM cells. Thus, their direct regulation on chromatin is unlikely to be due to a direct physical interaction.

◀ Fig. 3 BLIMP1 KD and EZH2 inhibition induce overlapping transcriptional changes. **a** RNAseq results for 48 h-induced RP cells comparing *PmiR2* to *NtmiR*. Values are plotted as \log_2 fold change vs. $-\log_{10}(q$ value). Red indicates those genes with a q value ≤ 0.05 and a \log_2 fold change ≤ -0.3 or ≥ 0.3 . Heat maps depicting the Z-score of the \log_2 fold change comparing *PmiR2* to *NtmiR* for three independent replicates looking at **(b)** B cell genes and **(c)** apoptosis genes. **d** RNAseq results for RP cells treated for 48 h with 300 nM tazemetostat compared to vehicle control (DMSO). **e** Overlapping genes with increased expression following *PRDM1* KD or tazemetostat treatment. **f** Overlapping genes with decreased expression following *PRDM1* KD or tazemetostat treatment. Overlaps tested using Fisher's exact test. **g** Overlaps of genes significantly induced by both BLIMP1 KD and tazemetostat with Hallmarks gene sets from the molecular signatures database, showing the top 10 most significantly overlapping gene sets.

The known DNA binding motif for BLIMP1 [55] was enriched by de novo motif analysis in the BLIMP1 peaks for all three cell lines (Fig. S4F) and the BLIMP1 ChIPseq signals were enriched at proximal positions relative to their assigned transcription start sites (TSSs) (Fig. S4G). Comparing the distribution of BLIMP1 peaks in OPM-2 and NCI-H929 to the RP cell line (Fig. S4H), showed that BLIMP1 binds to largely the same sites in WM and MM cells.

An analysis [50, 51] of genes assigned to H3K27me3 peaks revealed similar gene sets marked by H3K27me3 in all three cell lines (Fig. S5A). Interestingly, TNF α and IL2/STAT5 signalling genes were amongst the most highly enriched in the RP but not the myeloma cells. The myeloma cell lines displayed a much stronger enrichment of H3K27me3 over TSSs than the RP cells (Fig. S5B), indicating that H3K27me3 is more often present at gene distal sites in RP cells than myeloma cells. EZH2 was also highly enriched just downstream of TSSs in NCI-H929 cells (Fig. S5C). Correspondingly, we observed low enrichment of the H3K27me3 mark in the OPM-2 and NCI-H929 cell lines over sites marked by H3K27me3 in the RP cell line (Fig. S5D).

To identify the direct transcriptional targets of BLIMP1 and EZH2, we compared our ChIPseq and transcriptome profiling data from the RP cell line. There were 231 and 120 genes associated with BLIMP1 binding that were either induced or repressed upon BLIMP1 KD respectively (Fig. 4f, g). Conversely, 118 genes were both induced upon tazemetostat treatment and associated with the H3K27me3 mark (Fig. 4h), but only seven genes with decreased expression were marked by H3K27me3 (Fig. 4i). Overall, only 3% of genes marked by H3K27me3 were de-repressed following tazemetostat treatment, indicating that inhibition of EZH2's catalytic activity alone is insufficient to activate most H3K27me3 targets over 48 h. Meanwhile, approximately one-third of BLIMP1-bound genes showed altered expression upon BLIMP1 KD, indicating that BLIMP1 binding actively maintains gene repression. Taken together,

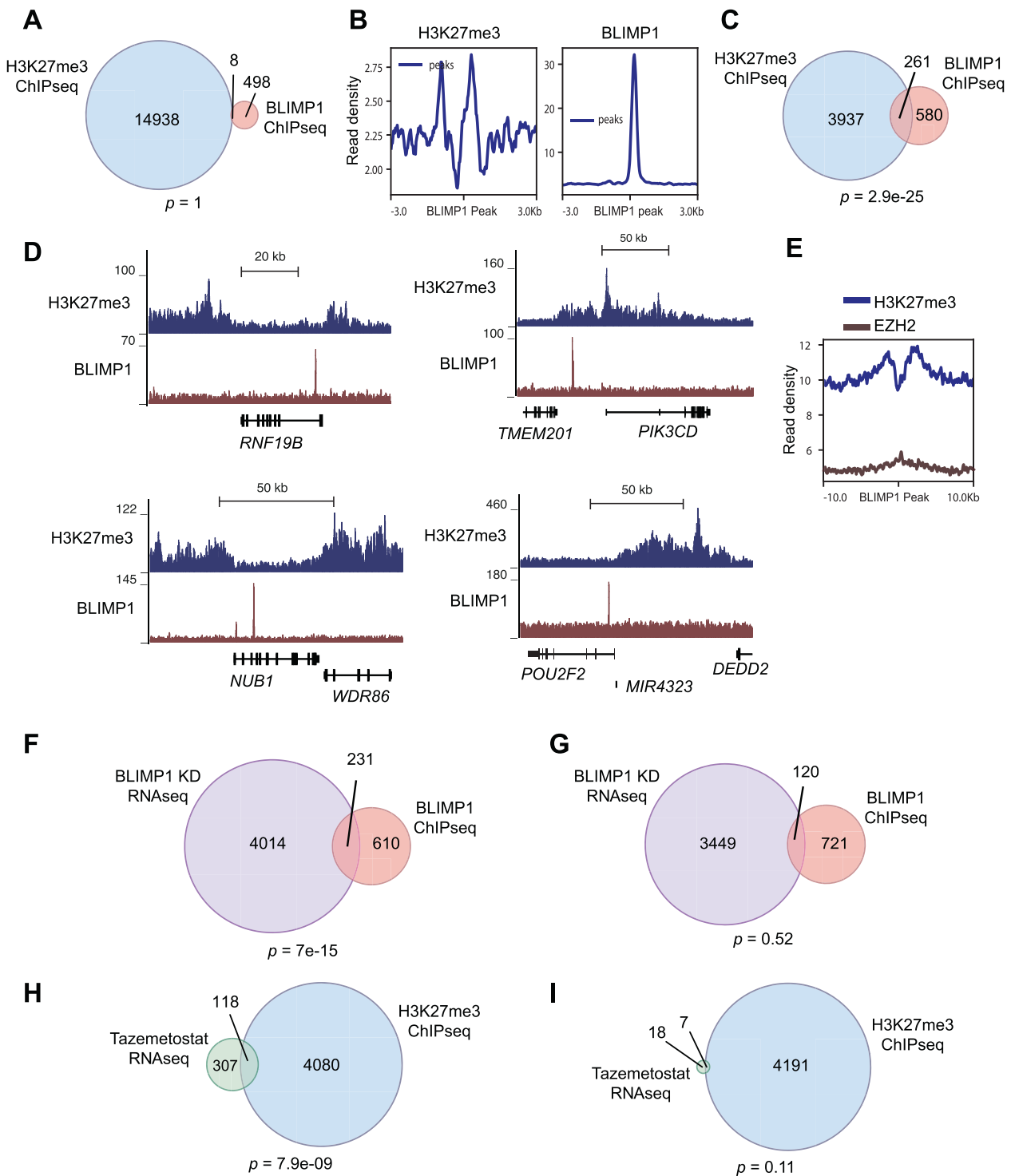
as BLIMP1 and H3K27me3 are largely present at distinct sites from one another, most of their overlapping effects on transcription are likely through their binding to the same genes at distinct sites, as well as BLIMP1 maintenance of EZH2 protein levels.

A subset of BLIMP1 targets are regulated via EZH2

A number of genes repressed by BLIMP1 bore both BLIMP1 and H3K27me3, such as *PIK3CD*, *POU2F2* (Fig. 4d) and *ZFP36L1* (Fig. 5a). Meanwhile, others bore only H3K27me3, but not BLIMP1, including *RCAN3*, *TNFRSF14* and *CIITA* (Fig. 5b–d). Yet others such as *TFEC* were bound by BLIMP1 alone (Fig. 5e). We therefore asked whether the genes bearing H3K27me3 are repressed by BLIMP1 via the maintenance of EZH2. By overexpressing EZH2 in RP cells upon BLIMP1 KD, we performed RT-qPCR and observed that repression of the genes *RCAN3* and *ZFP36L1* was restored, as well as the repression of the immune inhibitory checkpoint ligand/receptor gene *TNFRSF14* [56] and the inhibitory receptor gene *HAVCR2* [57] (Fig. 5f). By comparison, BLIMP1 binding targets not bearing H3K27me3 such as *TFEC* were not altered upon EZH2 restoration. Thus, a subset of BLIMP1 targets are regulated through EZH2 maintenance and can be identified by the H3K27me3 mark.

BLIMP1 represses transcription of immune surveillance and signalling molecules in concert with EZH2

Further analysis of the highly enriched immune signalling genes differentially expressed upon BLIMP1 KD identified three mechanistic categories. First, BLIMP1 represses the expression of genes encoding surface ligands that can activate T and NK cells, including *ICOSLG*, *TNFSF9*, *CD48*, *MICA*, *CLEC2B*, *ICAM1* and *ITGAM*, and MHC class II molecules including *HLA-DMA*, *HLA-DMB* and *CD1D* (Fig. 6a). Second, BLIMP1 represses genes encoding both immune-checkpoint inhibitory ligands and their corresponding receptors, including the receptor-ligand pairs *TNFRSF14* and *BTLA*, as well as *LAG3* and *LGALS3*. Furthermore, the inhibitory receptor gene *LILRB1*, whose loss promotes immune escape in myeloma [58] is repressed by BLIMP1. Additionally, the gene encoding the inhibitory ligand PD-L2 is repressed, with BLIMP1 binding just downstream of *PDCDLG2* (Fig. S6A). Notably, repression of inhibitory ligands and receptors could promote or inhibit immune escape from tumour immune surveillance. The third mechanistic category includes interferon and TNF α signalling genes. The receptor-encoding genes *IFNGRI*, *IFNARI*, *IFNLR1*, *TNFRSF1A* and *TNFRSF1B* are de-repressed upon BLIMP1 KD, as well as downstream players in interferon



signalling, *JAK1*, *STAT1*, *STAT2*, *IRF9*, *IFIT1-3*, *OAS1-3*, and TNF pathway members *MAP3K5*, *CASP8* and *CASP9*, which are also apoptosis mediators (Fig. 3c). Beyond these categories, MHC class I genes, *HLA-A* and *HLA-B* which can both mediate inhibition of NK-cell immune surveillance, are induced by BLIMP1, in contrast to previous studies [54, 59].

Around half of the genes identified above were also significantly changed with tazemetostat treatment, including *CD48*, *LILRB1*, *LGALS3*, *PDCD1LG2* and *STAT1* (Fig. S6B). Interestingly, while none of the surface molecule genes except for *PDCD1LG2* were bound by BLIMP1, some were enriched for H3K27me3 (Fig. 6b). Whereas the downstream signalling effectors, *IFIT2* and *STAT1*, were

◀ Fig. 4 BLIMP1 binds at a distance to the H3K27me3 mark. **a** Venn diagram of H3K27me3 and BLIMP1 peaks extended ± 500 bp, showing overlaps in these regions. $p = 1$, not significant as determined by hypergeometric test. Called peaks determined by overlap from peak calling from two independent experiments. **b** Enrichment of signal from ChIPseq tracks ± 3 kb from the centre of BLIMP1 binding sites. Data depicts representative experiment of two biological replicates. **c** Venn diagram of genes assigned to H3K27me3 and BLIMP1 peaks showing overlapping genes. $p = 2.9 \times 10^{-25}$ as determined by Fisher's exact test. **d** ChIPseq tracks for H3K27me3 and BLIMP1 in the RP cell line. Data represents combination of reads from two independent experiments. **e** Enrichment of signal from ChIPseq tracks ± 10 kb from the centre of BLIMP1 binding sites in the NCI-H929 cell line. **f** Venn diagram depicting the overlap in genes with significantly increased expression following BLIMP1 KD and genes assigned to BLIMP1 binding sites. $p = 7 \times 10^{-15}$, as determined by Fisher's exact test. **g** Venn diagram depicting the overlap in genes with significantly decreased expression following BLIMP1 KD and genes assigned to BLIMP1 binding sites. $p = 0.52$, not significant as determined by Fisher's exact test. **h** Venn diagram depicting genes with significantly increased expression following tazemetostat treatment overlapping with genes assigned to H3K27me3 peaks. $p = 7.9 \times 10^{-9}$, as determined by Fisher's exact test. **i** Venn diagram depicting genes with significantly decreased expression following tazemetostat treatment overlapping with genes assigned to H3K27me3 peaks. $p = 0.11$, not significant, as determined by Fisher's exact test. All ChIPseq experiments were performed as two biological replicates.

bound by BLIMP1 (Fig. 6c), consistent with previous findings [60]. A number of these differentially expressed genes did not bear either H3K27me3 or BLIMP1, and their expression changes are therefore likely secondary effects downstream of EZH2 and BLIMP1. Taken together, BLIMP1 and EZH2 repress the transcription of genes encoding mediators of killing by NK or T cells when expressed on target cells, NK- and T-cell inhibitory receptors and their ligands, as well as cytokine receptors and downstream signal propagation genes.

BLIMP1 and EZH2 confer evasion from NK cell-mediated cytotoxicity

The transcriptional changes above suggest that BLIMP1 and EZH2 potentially mediate escape from tumour immune surveillance. We therefore hypothesised that the loss of BLIMP1 protein or EZH2 activity in RP cells could lead to changes in NK cell-mediated cytotoxicity. We isolated NK cells from human blood and co-cultured them with RP cells after BLIMP1 KD or tazemetostat treatment and measured the surface expression of the degranulation marker LAMP-1 (also called CD107a) on NK cells by flow cytometry. This revealed a 1.5-fold increase in frequency of LAMP-1⁺ NK cells upon co-culture with *PmiR1* compared to *NTmiR* RP cells, showing that the loss of BLIMP1 sensitises NK cells to activation by RP cells (Fig. 6d, e and S6C). Tazemetostat-treated RP cells did not increase NK cell degranulation (Fig. S6D, E). Strikingly though, both

BLIMP1 KD and tazemetostat treatment resulted in increased NK cell-mediated cytotoxicity of RP cells, although the response to *PmiR2* cells did not reach statistical significance, presumably due to *PmiR2* cells having lower extent of BLIMP1 KD, or due to NK-cell donor variability since NK-cells from one donor out of four failed to show an altered response (Fig. 6f). RP cells subjected to conditioned media from either *PmiR1*- or *PmiR2*-expressing RP cells showed unaltered effects on NK-cell degranulation or cytolytic activity compared with *NTmiR* cell media (Fig. S6F, G), again showing that the effect is autonomous to BLIMP1 KD cells. Collectively, these data indicate that BLIMP1 and EZH2 might mediate the escape from NK-cell surveillance, with BLIMP1 both suppressing NK cell activation and the resultant WM cell cytotoxicity, whereas EZH2 suppresses the cytolytic response of the WM cell line.

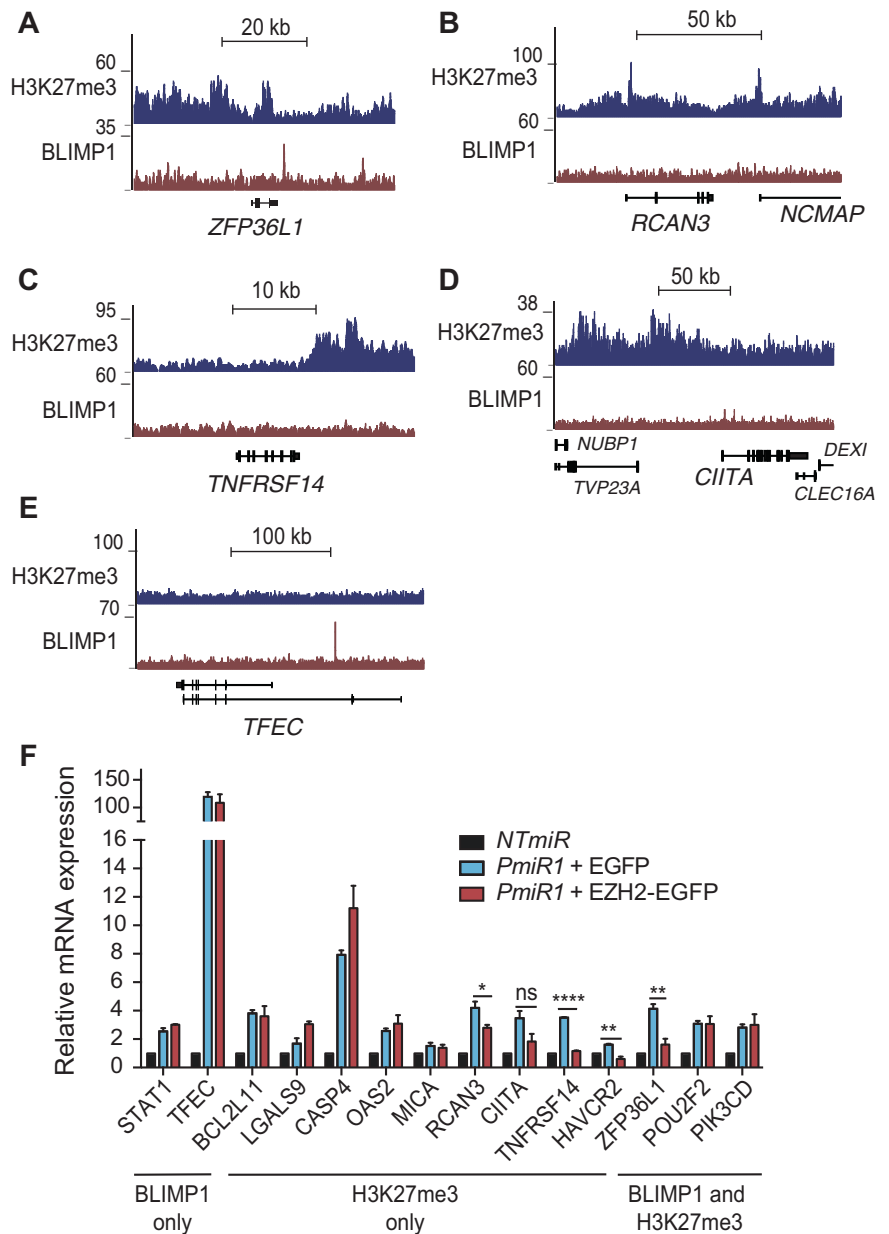
Discussion

In this study, we used WM cell line models to show for the first time that the plasma cell master regulator BLIMP1 has a crucial role in the survival of cells from these models. We further show that BLIMP1 maintains the protein levels of the histone methyltransferase EZH2, demonstrating a more complex functional interaction between BLIMP1 and EZH2 than previously thought [16, 31–33]. Furthermore, we show that the factors repress the expression of immune signalling genes, including immune checkpoint inhibitory ligands and their receptors, indicating that the factors may be involved in the evasion of malignant lymphoplasmacytic cells from tumour immune surveillance. Consistent with this, we observed enhanced degranulation of NK cells in response to RP cells upon loss of BLIMP1, and enhanced NK cell-mediated RP cell cytotoxicity upon either BLIMP1 depletion or EZH2 inhibition.

Rituximab is a first line of treatment in WM, targeting the B cell specific surface molecule CD20 at least in part through NK cell engagement [61]. However, clonal plasma cells remaining after this treatment present a formidable challenge in WM therapy [62]. Furthermore, rituximab is not recommended for patients exhibiting high serum IgM levels [63], due to the risks of an IgM 'flare' following treatment [64]. The RP cell line used in this study has a more uniform and differentiated cellular profile than what is characteristic for WM tumours, reflecting the fact that RP cells are derived from a late-stage WM patient who had developed rituximab resistance [65].

While less-differentiated lymphoplasmacytic cells constitute the majority of the tumour burden in WM [66], the concern of IgM-related symptoms and the presence of residual plasma cells after rituximab treatment highlight the

Fig. 5 BLIMP1 regulates a subset of target genes via EZH2. ChIPseq tracks for H3K27me3 and BLIMP1 over the genes (a) *ZFP36L1*, (b) *RCAN3*, (c) *TNFRSF14*, (d) *CIITA*, and (e) *TPEC*. f Bar graph depicting RT-qPCR experiments in RP cells expressing *NTmiR* or *PmiR1* with EGFP or EZH2-EGFP, with *ACTB* used as a normalisation gene. The selected target genes bear peaks for either BLIMP1, H3K27me3 or both factors. All *p* values as determined by student's two-tailed *t* test. (ns) $p > 0.05$; * $p \leq 0.05$; ** $p \leq 0.01$; **** $p \leq 0.0001$. The bar graph was plotted as the mean of three independent experiments with error bars representing standard deviation.



importance of the antibody-secreting CD20^{low} or negative plasma cell compartment in WM [62, 67]. As such, the plasma cell-like RP cells provide a heuristic model for WM plasma cells, with the caveat of being highly proliferative, perhaps more reminiscent of plasmablasts than bona fide plasma cells, with recent studies revealing a role for EZH2 together with BLIMP1 in the differentiation of plasmablasts upon T-independent stimulation [16, 31, 68]. Although WM plasma cells are not highly proliferative [69–71], our results are valuable to inform more direct studies into WM by providing potential insights into the molecular mechanisms regulating the plasma cell compartment which is increasingly being recognised for its clinical and pathogenic significance [72].

Immune evasion is crucial in lymphomas, although both normal and malignant lymphocytes regularly interact with immune effectors [73]. In WM, secreted PD-1 ligands inhibit T cell responses [74], but other mechanisms of immune evasion have not been investigated. Our results provide a link between BLIMP1 and EZH2 and evasion from NK cell-mediated cytotoxicity in vitro, providing an avenue for further study of the involvement of the factors in the evasion from tumour surveillance in vivo. Based on our transcriptomic profiling, BLIMP1 likely suppresses NK cell responses by mediating target cell “hiding” through repressing activating ligands and MHC class I molecules. Conversely, EZH2 is more likely to be de-sensitising target cells to external cytotoxicity-inducing signals, perhaps by

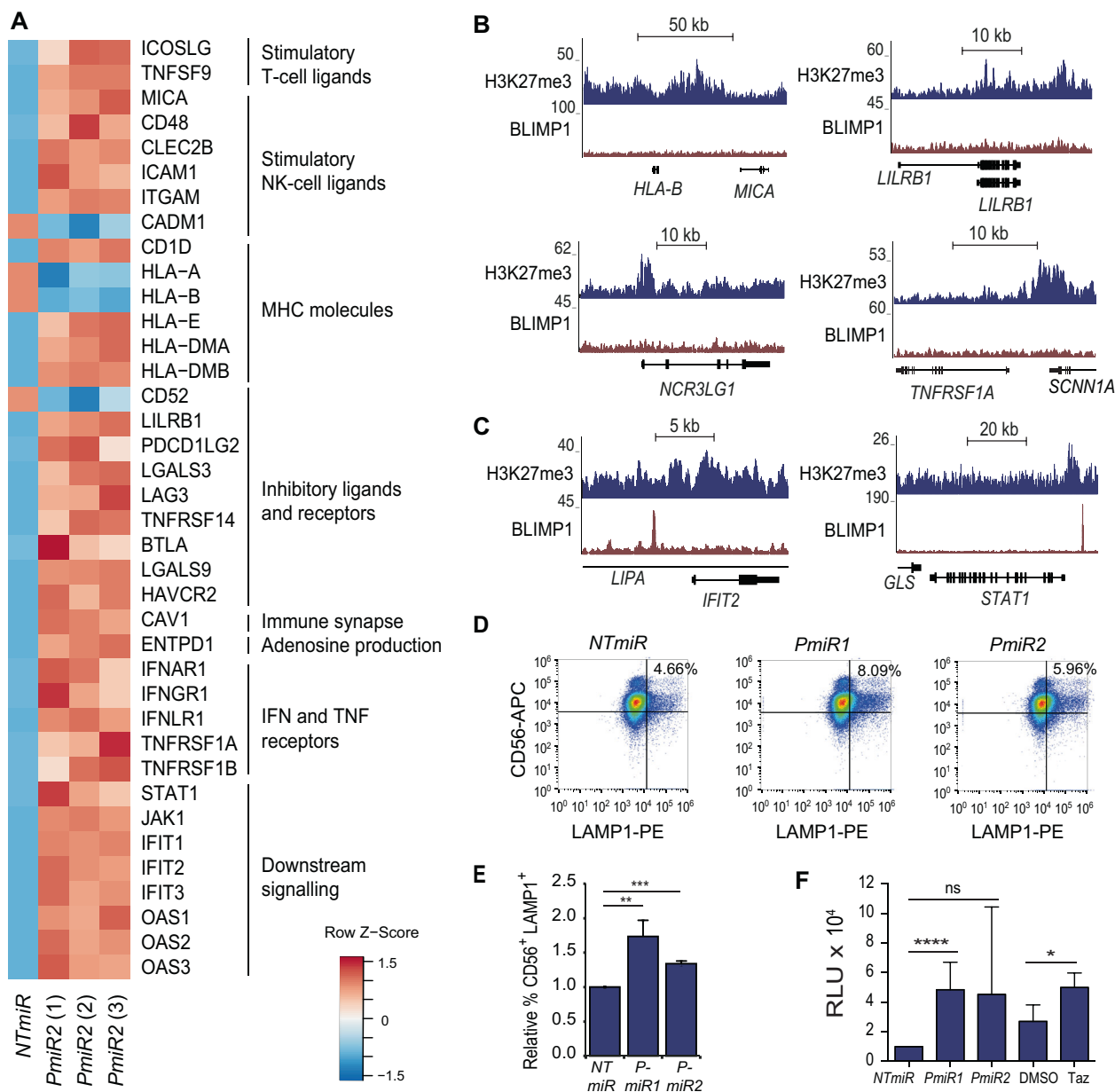


Fig. 6 BLIMP1 and EZH2 promote WM tumour immune evasion.

a Heat maps showing z-score of the \log_2 fold change for *PmiR2* compared to *NTmiR* in RP cells with three independent replicates looking at genes encoding proteins involved in the stimulation of T and NK cells, MHC molecules, inhibitory ligands and receptors, IFN and TNF receptors and downstream signalling. ChIPseq tracks for H3K27me3 and BLIMP1 in the RP cell line over **(b)** the immune surface molecule genes *HLA-B*, *MICA*, *LILRB1*, *NCR3LG1*, *TNFRSF1A*, or **(c)** the downstream signalling genes, *IFIT2* and *STAT1*. Data represents a combination of reads from two independent experiments. **d** Scatter plots showing the percentage of CD56⁺LAMP1⁺ cells (upper right quadrants) representing degranulating NK cells, as determined by flow cytometry following co-culture with *NTmiR*, *PmiR1* or *PmiR2* expressing RP cells. One representative

experiment is displayed. **e** Relative quantification of the degranulation assay showing the average of NK-cell degranulation from 8 individual donors for *NTmiR* and *PmiR1* expressing cells and four independent donors for *PmiR2* expressing RP cells. **f** Cytotoxicity depicted in relative luminescence units (RLU), as measured by adenylate kinase activity in the culture media following 4 h co-culture of NK cells with RP cells expressing *NTmiR* or *PmiR1*, or RP cells treated with DMSO or 1 μ M Tazemetostat. Cells were co-cultured at the effector:target ratio of 20:1. Results of the degranulation and cytotoxicity assays from four individual donors, performed in two pairs on two separate occasions. All *p* values as determined by student's two-tailed *t* test. (ns) *p* > 0.05; **p* ≤ 0.05; ***p* ≤ 0.01; ****p* ≤ 0.001; *****p* ≤ 0.0001. All graphs were plotted as the mean of independent experiments with error bars representing standard deviation.

repressing pro-apoptotic gene expression. Interestingly, in melanoma EZH2 promotes evasion from IFN γ -producing cytotoxic T cells [75]. This finding together with our current

study make EZH2 an interesting potential target for chemical sensitisation of WM and other tumours to immune-cell mediated killing.

In conclusion, we provide evidence for a crucial role of BLIMP1 in promoting survival of cells from WM cell lines and show that BLIMP1 maintains EZH2 protein levels in both WM and MM cell lines. We further reveal a cooperation between BLIMP1 and EZH2 in the repression of immune surveillance genes, and find that BLIMP1 and EZH2 confer evasion from NK-cell mediated cytotoxicity, a finding that will be important to expand to future *in vivo* studies where more complex immune interactions can be tested.

Materials and methods

Cloning

For KD of BLIMP1, artificial miRNA sequences were designed to target the *PRDM1* transcript using the RNAi-Designer tool (Thermo Fisher Scientific). These were named *PmiR1* and *PmiR2*. A non-targeting control miRNA (*NTmiR*) was also used as previously described [76]. The miRNA sequences (Table S20) were cloned into the tetracycline-inducible pPB-hCMV*1-miR plasmid [76, 77].

ChIPseq

Transcription factor ChIP for BLIMP1 and EZH2 was performed as previously described [32, 78, 79]. Histone ChIP for pan-H3 and the H3K27me3 mark was performed as previously described [48].

NK cell isolation

NK cells were isolated from heparinised buffy coats obtained from healthy human donors, who all provided informed consent, provided by the Icelandic Blood Bank (ethical approval #06-068).

Further “Materials and Methods” including all primer sequences (Tables S21–22) are described in Supplementary Information.

Data availability

RNAseq and ChIPseq data are available at <http://www.ebi.ac.uk/arrayexpress/experiments/E-MTAB-7739> under the accession code: E-MTAB-7739.

Acknowledgements We thank deCODE Genetics/Amgen for the high throughput sequencing, Arnar Pálsson and Dagný A. Rúnarsdóttir for their advice on RNAseq data analysis, Árni Ásbjarnarson for technical assistance on western blot analysis, Jóna Freysdóttir and Sunnefa Yeatman Ómarsdóttir for their advice on the isolation of NK cells, and the group of Eiríkur Steingrímsson for useful discussions and advice on the project. We thank Helga M. Ögmundsdóttir for advice and

helpful discussions on the manuscript and we thank Dr. Roopsha Sengupta for providing critical inputs and proof-reading the manuscript.

Funding This work was supported by project grants from the Icelandic Research Fund (grant no. 140950-051) and the Icelandic Cancer Society, a doctoral fellowship from the University of Iceland, and grant from the University of Iceland Eggertssjodur and funds from the COST Project EpiChemBio.

Compliance with ethical standards

Conflict of interest The authors declare that they have no conflict of interest.

Publisher's note Springer Nature remains neutral with regard to jurisdictional claims in published maps and institutional affiliations.

References

- Kyle RA, Larson DR, McPhail ED, Therneau TM, Dispenzieri A, Kumar S, et al. Fifty-year incidence of Waldenstrom Macroglobulinemia in Olmsted County, Minnesota, from 1961 through 2010: a population-based study with complete case capture and hematopathologic review. *Mayo Clin Proc.* 2018;93:739–46.
- Wang H, Chen Y, Li F, Delasalle K, Wang J, Alexanian R, et al. Temporal and geographic variations of Waldenstrom macroglobulinemia incidence: a large population-based study. *Cancer.* 2012;118:3793–800.
- Iwanaga M, Chiang CJ, Soda M, Lai MS, Yang YW, Miyazaki Y, et al. Incidence of lymphoplasmacytic lymphoma/Waldenstrom's macroglobulinaemia in Japan and Taiwan population-based cancer registries, 1996–2003. *Int J Cancer.* 2014;134:174–80.
- Vijay A, Gertz MA. Waldenström macroglobulinemia. *Blood.* 2007;109:5096–103.
- Treon SP. How I treat Waldenström macroglobulinemia. *Blood.* 2009;114:2375.
- Treon SP, Xu L, Yang G, Zhou Y, Liu X, Cao Y, et al. MYD88 L265P somatic mutation in Waldenström's Macroglobulinemia. *N Engl J Med.* 2012;367:826–33.
- Xu L, Hunter ZR, Yang G, Cao Y, Liu X, Manning R, et al. Detection of MYD88 L265P in peripheral blood of patients with Waldenström's Macroglobulinemia and IgM monoclonal gammopathy of undetermined significance. *Leukemia.* 2014;28:1698.
- Yu X, Li W, Deng Q, Li L, Hsi ED, Young KH, et al. MYD88 L265P mutation in lymphoid malignancies. *Cancer Res.* <https://doi.org/10.1158/0008-5472.CAN-18-0215> 2018.
- Ren B, Chee KJ, Kim TH, Maniatis T. PRDI-BF1/Blimp-1 repression is mediated by corepressors of the Groucho family of proteins. *Genes Dev.* 1999;13:125–37.
- Yu J, Angelin-Duclos C, Greenwood J, Liao J, Calame K. Transcriptional repression by Blimp-1 (PRDI-BF1) involves recruitment of histone deacetylase. *Mol Cell Biol.* 2000;20:2592–603.
- Györy I, Wu J, Fejér G, Seto E, Wright KL. PRDI-BF1 recruits the histone H3 methyltransferase G9a in transcriptional silencing. *Nat Immunol.* 2004;5:299.
- Piskurich JF, Lin KI, Lin Y, Wang Y, Ting JPY, Calame K. BLIMP-1 mediates extinction of major histocompatibility class II transactivator expression in plasma cells. *Nat Immunol.* 2000;1:526.
- Tooze RM, Stephenson S, Doody GM. Repression of IFN- γ induction of class II transactivator: a role for PRDM1/Blimp-1 in regulation of cytokine signaling. *J Immunol.* 2006;177:4584–93.

14. Shaffer AL, Lin K-I, Kuo TC, Yu X, Hurt EM, Rosenwald A, et al. Blimp-1 orchestrates plasma cell differentiation by extinguishing the mature B cell gene expression program. *Immunity*. 2002;17:51–62.
15. Tellier J, Shi W, Minnich M, Liao Y, Crawford S, Smyth GK, et al. Blimp-1 controls plasma cell function through the regulation of immunoglobulin secretion and the unfolded protein response. *Nat Immunol*. 2016;17:323.
16. Minnich M, Tagoh H, Bönelt P, Axelsson E, Fischer M, Cebolla B, et al. Multifunctional role of the transcription factor Blimp-1 in coordinating plasma cell differentiation. *Nat Immunol*. 2016;17:331.
17. Lin F-R, Kuo H-K, Ying H-Y, Yang F-H, Lin K-I. Induction of apoptosis in plasma cells by B lymphocyte-induced maturation protein-1 knockdown. *Cancer Res*. 2007;67:11914. <https://doi.org/10.1158/0008-5472.CAN-07-1868>.
18. Shapiro-Shelef M, Lin K-I, McHeyzer-Williams LJ, Liao J, McHeyzer-Williams MG, Calame K. Blimp-1 is required for the formation of immunoglobulin secreting plasma cells and pre-plasma memory B cells. *Immunity*. 2003;19:607–20.
19. Kallies A, Hasbold J, Fairfax K, Pridans C, Emslie D, McKenzie BS, et al. Initiation of plasma-cell differentiation is independent of the transcription factor Blimp-1. *Immunity*. 2007;26:555–66.
20. Pasqualucci L, Compagno M, Houldsworth J, Monti S, Grunn A, Nandula SV, et al. Inactivation of the PRDM1/BLIMP1 gene in diffuse large B cell lymphoma. *J Exp Med*. 2006;203:311.
21. Mandelbaum J, Bhagat G, Tang H, Mo T, Brahmachary M, Shen Q, et al. BLIMP1 is a tumor suppressor gene frequently disrupted in activated B cell-like diffuse large B cell lymphoma. *Cancer Cell*. 2010;18:568–79.
22. Calado DP, Zhang B, Srinivasan L, Sasaki Y, Seagal J, Unitt C, et al. Constitutive canonical NF- κ B activation cooperates with disruption of BLIMP1 in the pathogenesis of activated B cell-like diffuse large cell lymphoma. *Cancer Cell*. 2010;18:580–9.
23. Schop RFJ, Kuehl WM, Van Wier SA, Ahmann GJ, Price-Troska T, Bailey RJ, et al. Waldenström macroglobulinemia neoplastic cells lack immunoglobulin heavy chain locus translocations but have frequent 6q deletions. *Blood*. 2002;100. <https://doi.org/10.1182/blood.V100.8.2996>.
24. Roberts MJ, Chadburn A, Ma S, Hyjek E, Peterson LC. Nuclear protein dysregulation in lymphoplasmacytic lymphoma/Waldenström macroglobulinemia. *Am J Clin Pathol*. 2013;139:210–9.
25. Zhou Y, Liu X, Xu L, Hunter ZR, Cao Y, Yang G, et al. Transcriptional repression of plasma cell differentiation is orchestrated by aberrant over-expression of the ETS factor SPIB in Waldenström macroglobulinemia. *Br J Haematol*. 2014;166:677–89.
26. Savitsky D, Calame K. B-1 B lymphocytes require Blimp-1 for immunoglobulin secretion. *J Exp Med*. 2006;203:2305.
27. Morgan MAJ, Magnusdottir E, Kuo TC, Tunyaplin C, Harper J, Arnold SJ, et al. Blimp-1/Prdm1 alternative promoter usage during mouse development and plasma cell differentiation. *Mol Cellular Biol*. 2009;29:5813. <https://doi.org/10.1128/MCB.00670-09>.
28. Pasare C, Medzhitov R. Control of B-cell responses by toll-like receptors. *Nature*. 2005;438:364.
29. Hunter ZR, Xu L, Yang G, Tsakmaklis N, Vos JM, Liu X, et al. Transcriptome sequencing reveals a profile that corresponds to genomic variants in Waldenström macroglobulinemia. *Blood*. 2016;128:827–38. <https://doi.org/10.1182/blood-2016-03-708263>.
30. Treon SP, Cao Y, Xu L, Yang G, Liu X, Hunter ZR. Somatic mutations in MYD88 and CXCR4 are determinants of clinical presentation and overall survival in Waldenström macroglobulinemia. *Blood*. 2014;123:2791.
31. Guo M, Price MJ, Patterson DG, Barwick BG, Haines RR, Kania AK, et al. EZH2 represses the B cell transcriptional program and regulates antibody-secreting cell metabolism and antibody production. *J Immunol*. 2018;200:1039–52.
32. Magnúsdóttir E, Dietmann S, Murakami K, Günesdogan U, Tang F, Bao S, et al. A tripartite transcription factor network regulates primordial germ cell specification in mice. *Nat Cell Biol*. 2013;15:905.
33. Kurimoto K, Yabuta Y, Hayashi K, Ohta H, Kiyonari H, Mitani T, et al. Quantitative dynamics of chromatin remodeling during germ cell specification from mouse embryonic stem cells. *Cell Stem Cell*. 2015;16:517–32.
34. Müller J, Hart CM, Francis NJ, Vargas ML, Sengupta A, Wild B, et al. Histone methyltransferase activity of a drosophila polycomb group repressor complex. *Cell*. 2002;111:197–208.
35. Czermin B, Melfi R, McCabe D, Seitz V, Imhof A, Pirrotta V. Drosophila enhancer of Zeste/ESC complexes have a histone H3 methyltransferase activity that marks chromosomal polycomb sites. *Cell*. 2002;111:185–96.
36. Carroll D, Erhardt S, Pagani M, Barton SC, Surani MA, Jenuwein T. The polycomb-group gene *Ezh2* is required for early mouse development. *Mol Cell Biol*. 2001;21:4330.
37. Morin RD, Johnson NA, Severson TM, Mungall AJ, An J, Goya R, et al. Somatic mutations altering EZH2 (Tyr641) in follicular and diffuse large B-cell lymphomas of germinal-center origin. *Nat Genet*. 2010;42:181.
38. Pawlyn C, Bright MD, Buros AF, Stein CK, Walters Z, Aronson LI, et al. Overexpression of EZH2 in multiple myeloma is associated with poor prognosis and dysregulation of cell cycle control. *Blood Cancer J*. 2017;7:e549.
39. Hernando H, Gelato KA, Lesche R, Beckmann G, Koehr S, Otto S, et al. EZH2 inhibition blocks multiple myeloma cell growth through upregulation of epithelial tumor suppressor genes. *Mol Cancer Ther*. 2016;15:287.
40. Roccaro AM, Sacco A, Jia X, Azab AK, Maiso P, Ngo HT, et al. microRNA-dependent modulation of histone acetylation in Waldenström macroglobulinemia. *Blood*. 2010; blood-2010-2001-265686.
41. Garcia JF, Roncador G, Garcia JF, Sanz AI, Maestre L, Lucas E, et al. PRDM1/BLIMP-1 expression in multiple B and T-cell lymphoma. *Haematologica*. 2006;91:467.
42. Lois C, Hong EJ, Pease S, Brown EJ, Baltimore D. Germline transmission and tissue-specific expression of transgenes delivered by lentiviral vectors. *Science*. 2002;295:868–72.
43. Kallies A, Hasbold J, Tarlinton DM, Dietrich W, Corcoran LM, Hodgkin PD, et al. Plasma cell ontogeny defined by quantitative changes in Blimp-1 expression. *J Exp Med*. 2004;200:967.
44. Piskurich JF, Lin K-I, Lin Y, Wang Y, Ting JP-Y, Calame K. BLIMP-1 mediates extinction of major histocompatibility class II transactivator expression in plasma cells. *Nat Immunol*. 2000;1:526.
45. Chen H, Gilbert CA, Hudson JA, Bolick SC, Wright KL, Piskurich JF. Positive regulatory domain I-binding factor 1 mediates repression of the MHC class II transactivator (CIITA) type IV promoter. *Mol Immunol*. 2007;44:1461–70.
46. Lin K-I, Angelin-Duclos C, Kuo TC, Calame K. Blimp-1-dependent repression of Pax-5 is required for differentiation of B cells to immunoglobulin M-secreting plasma cells. *Mol Cell Biol*. 2002;22:4771–80.
47. Lin Y, Wong K-k, Calame K. Repression of c-myc transcription by Blimp-1, an inducer of terminal B cell differentiation. *Science*. 1997;276:596–9.
48. Shaffer AL, Emre NCT, Lamy L, Ngo VN, Wright G, Xiao W, et al. IRF4 addiction in multiple myeloma. *Nature*. 2008;454:226.
49. Petermann F, Pekowska A, Johnson CA, Nankovic D, Shih HY, Jiang K, et al. The magnitude of IFN-gamma responses is fine-tuned by DNA architecture and the non-coding transcript of *Ifngas1*. *Mol Cell*. 2019;75:1229–1242.e1225.

50. Subramanian A, Tamayo P, Mootha VK, Mukherjee S, Ebert BL, Gillette MA, et al. Gene set enrichment analysis: a knowledge-based approach for interpreting genome-wide expression profiles. *Proc Natl Acad Sci*. 2005;102:15545.
51. Liberzon A, Birger C, Thorvaldsdottir H, Ghandi M, Mesirov JP, Tamayo P. The molecular signatures database (MSigDB) hallmark gene set collection. *Cell Syst*. 2015;1:417–25.
52. Elias S, Robertson EJ, Bikoff EK, Mould AW. Blimp-1/PRDM1 is a critical regulator of Type III Interferon responses in mammary epithelial cells. *Sci Rep*. 2018;8:237–237.
53. Hung KH, Su ST, Chen CY, Hsu PH, Huang SY, Wu WJ, et al. Aiolos collaborates with Blimp-1 to regulate the survival of multiple myeloma cells. *Cell Death Differ*. 2016;23:1175.
54. Doody GM, Stephenson S, McManamy C, Tooze RM. PRDM1/BLIMP-1 modulates IFN- γ -dependent control of the MHC class I antigen-processing and peptide-loading pathway. *J Immunol*. 2007;179:7614. <https://doi.org/10.4049/jimmunol.179.11.7614>.
55. Kuo TC, Calame KLB. Lymphocyte-induced maturation protein (Blimp)-1, IFN regulatory factor (IRF)-1, and IRF-2 can bind to the same regulatory sites. *J Immunol*. 2004;173:5556.
56. Steinberg MW, Cheung TC, Ware CF. The signaling networks of the herpesvirus entry mediator (TNFRSF14) in immune regulation. *Immunological Rev*. 2011;244:169–87.
57. Anderson Ana C, Joller N, Kuchroo Vijay K. Lag-3, Tim-3, and TIGIT: co-inhibitory receptors with specialized functions in immune regulation. *Immunity*. 2016;44:989–1004.
58. Lozano E, Díaz T, Mena M-P, Suñe G, Calvo X, Calderón M, et al. Loss of the immune checkpoint CD85j/LILRB1 on malignant plasma cells contributes to immune escape in multiple myeloma. *J Immunol*. 2018;200:2581–91. [ji1701622](https://doi.org/10.1111/ji.1701622).
59. Mould AW, Morgan MAJ, Nelson AC, Bikoff EK, Robertson EJ. Blimp1/Prdm1 functions in opposition to Irf1 to maintain neonatal tolerance during postnatal intestinal maturation. *PLOS Genet*. 2015;11:e1005375.
60. Elias S, Robertson EJ, Bikoff EK, Mould AW. Blimp-1/PRDM1 is a critical regulator of Type III Interferon responses in mammary epithelial cells. *Sci Rep*. 2018;8:237.
61. Cartron G, Watier H, Golay J, Solal-Celigny P. From the bench to the bedside: ways to improve rituximab efficacy. *Blood*. 2004;104:2635.
62. Barakat FH, Medeiros LJ, Wei EX, Konoplev S, Lin P, Jorgensen JL. Residual monotypic plasma cells in patients with waldenström macroglobulinemia after therapy. *Am J Clin Pathol*. 2011;135:365–73.
63. Gavriatopoulou M, Musto P, Caers J, Merlini G, Kastritis E, van de Donk N, et al. European myeloma network recommendations on diagnosis and management of patients with rare plasma cell dyscrasias. *Leukemia*. 2018;32:1883–98.
64. Ghobrial IM, Fonseca R, Greipp PR, Blood E, Rue M, Vesole DH, et al. Initial immunoglobulin M 'flare' after rituximab therapy in patients diagnosed with Waldenström macroglobulinemia. *Cancer*. 2004;101:2593–8.
65. Paulus A, Chitta KS, Wallace PK, Advani PP, Akhtar S, Kuranz-Blake M, et al. Immunophenotyping of Waldenström's macroglobulinemia cell lines reveals distinct patterns of surface antigen expression: potential biological and therapeutic implications. *PloS one*. 2015;10:e0122338–e0122338.
66. Kriangkum J, Taylor BJ, Treon SP, Mant MJ, Belch AR, Pilarski LM. Clonotypic IgM V/D/J sequence analysis in Waldenström macroglobulinemia suggests an unusual B-cell origin and an expansion of polyclonal B cells in peripheral blood. *Blood*. 2004;104:2134. <https://doi.org/10.1182/blood-2003-11-4024>.
67. Varghese AM, Rawstron AC, Ashcroft AJ, Moreton P, Owen RG. Assessment of bone marrow response in Waldenström's Macroglobulinemia. *Clin Lymphoma Myeloma*. 2009;9:53–55.
68. Herviou L, Jourdan M, Martinez A-M, Cavalli G, Moreaux J. EZH2 is overexpressed in transitional preplasmablasts and is involved in human plasma cell differentiation. *Leukemia*. 2019;33:2047–60.
69. Morice WG, Chen D, Kurtin PJ, Hanson CA, McPhail ED. Novel immunophenotypic features of marrow lymphoplasmacytic lymphoma and correlation with Waldenström's macroglobulinemia. *Mod Pathol*. 2009;22:807–16.
70. Pasricha S-R, Juneja SK, Westerman DA, Came NA. Bone-marrow plasma cell burden correlates with IgM paraprotein concentration in Waldenström macroglobulinaemia. *J Clin Pathol*. 2011;64:520.
71. de Tute RM, Rawstron AC, Owen RG. Immunoglobulin M concentration in Waldenström macroglobulinemia: correlation with bone marrow B cells and plasma cells. *Clin Lymphoma Myeloma Leuk*. 2013;13:211–3.
72. El-Ayoubi A, Wang JQ, Hein N, Talaulikar D. Role of plasma cells in Waldenström macroglobulinaemia. *Pathology*. 2017;49:337–45.
73. de Charette M, Houot R. Hide or defend, the two strategies of lymphoma immune evasion: potential implications for immunotherapy. *Haematologica*. 2018;103:1256–68.
74. Jalali S, Price-Troska T, Paludo J, Villasboas J, Kim H-J, Yang Z-Z, et al. Soluble PD-1 ligands regulate T-cell function in Waldenström macroglobulinemia. *Blood Adv*. 2018;2:1985.
75. Zingg D, Arenas-Ramirez N, Sahin D, Rosalia RA, Antunes AT, Haeusel J, et al. The histone methyltransferase Ezh2 controls mechanisms of adaptive resistance to tumor immunotherapy. *Cell Rep*. 2017;20:854–67.
76. Hackett JA, Sengupta R, Zyllic JJ, Murakami K, Lee C, Down TA, et al. Germline DNA demethylation dynamics and imprint erasure through 5-hydroxymethylcytosine. *Science*. 2013;339:448–52.
77. Murakami K, Günesdogan U, Zyllic JJ, Tang WWC, Sengupta R, Kobayashi T, et al. NANOG alone induces germ cells in primed epiblast in vitro by activation of enhancers. *Nature*. 2016;529:403.
78. Boyer LA, Lee TI, Cole MF, Johnstone SE, Levine SS, Zucker JP, et al. Core transcriptional regulatory circuitry in human embryonic stem cells. *Cell*. 2005;122:947–56.
79. Magnúsdóttir E, Kalachikov S, Mizukoshi K, Savitsky D, Ishida-Yamamoto A, Panteleyev AA, et al. Epidermal terminal differentiation depends on B lymphocyte-induced maturation protein-1. *Proc Natl Acad Sci*. 2007;104:14988. <https://doi.org/10.1073/pnas.0707323104>.